Shared and Closed-Shell O−O Interactions in Silicates

G. V. Gibbs,[†] R. T. Downs,*[,‡] D. F. Cox,[§] N. L. Ross,[†] M. B. Boisen, Jr.,[||] and K. M. Rosso[⊥]

Department of Geosciences and Department of Chemical Engineering, Virginia Tech, Blacksburg, Virginia 24061, Department of Geosciences, University of Arizona, Tucson, Arizona 85721, Department of Mathematics, University of Idaho, Moscow, Idaho 83844-1103, and Chemical and Materials Science Division, and the W.R. Wiley Environmental Molecular Sciences Laboratory, Pacific Northwest National Laboratory, Richland, Washington 99352

Received: August 9, 2007; In Final Form: December 21, 2007

Bond paths of maximum electron density spanning O−O edges shared between equivalent or quasiequivalent MO_n ($n > 4$) coordination polyhedra are not uncommon electron density features displayed by silicates. On the basis of the positive values for the local electronic energy density, $H(\mathbf{r}_c)$, at the bond critical points, $\mathbf{r}_c$, they qualify as weak "closed-shell" interactions. As observed for M−O bonded interactions (M = first and second row metal atoms), the electron density, $\rho(\mathbf{r}_c)$, and the Laplacian of the electron density increase in a regular way as the separation between the O atoms, R(O−O), decreases. A simple model, based on R(O−O) and the distances of the Si atoms from the midpoint between adjacent pairs of O atoms, partitions the O−O bond paths in the high-pressure silica polymorph coesite into two largely disjoint domains, one with and one without bond paths. The occurrence of O−O bond paths shared in common between equivalent coordination polyhedra suggests that they may be grounded in some cases on factors other than bonded interactions, particularly since they are often displayed by inert procrystal representations of the electron density. In these cases, it can be argued that the accumulation of the electron density along the paths has its origin, at least in part, in the superposition of the peripheral electron density distributions of the metal M atoms occupying the edge-sharing polyhedra. On the other hand, the accumulation of electron density along the paths may stabilize a structure by shielding the adjacent M atoms in the edge-sharing polyhedra. For closed-shell Li−O, Na−O, and Mg−O interactions, $H(\mathbf{r}_c)$ is positive and increases as the value of $\rho(\mathbf{r}_c)$ increases, unlike the "shared" Be−O, B−O, C−O, Al−O, Si−O, P−O, and S−O interactions, where $H(\mathbf{r}_c)$ is negative and decreases as $\rho(\mathbf{r}_c)$ increases. The $H(\mathbf{r}_c)$ values for the weak closed-shell O−O interactions also increase as $\rho(\mathbf{r}_c)$ increases, as observed for the closed-shell M−O interactions. On the basis of the bond critical point properties and the negative $H(\mathbf{r}_c)$ value, the O−O interaction comprising the O_2 molecule in silica III qualifies as a shared interaction.

Introduction

A chemical bond is an undefined quantity, yet it has been discussed extensively in the scientific literature and particularly in textbooks as if it were a well-understood and simple concept. The core of the problem has been the inability of workers to define or at least to share a general consensus definition as to what constitutes a bond in a molecule or a crystal.[1] In an important step in resolving this problem, Runtz et al.[2] forged a model based on the topology of the electron density (ED) distribution in the internuclear region between a pair of potentially bonded atoms.[3] They found that the one property in the region that is most "bondlike" and resembles what might be considered to be characteristic of a bonded interaction is the presence of a pathway of maximum ED that links the pair. It has since been asserted that the presence of such a pathway (denoted a bond path) is a necessary and sufficient condition for a pair of atoms to be bonded in the chemical sense.[4,5] In addition to being a maximum value at each point along the path relative to that along any neighboring pathway, the ED decreases along paths of steepest descent starting at the local maxima at the nuclei of the bonded pair and extends along the path to the local minimum between the pair where the gradient of the ED, $\nabla\rho(\mathbf{r}) = 0$ (a stationary point defined as the bond critical point, $\mathbf{r}_c$,of the interaction), and the ED adopts a local minimum value parallel to the path. The properties (bond critical point properties) of the interaction at $\mathbf{r}_c$ are a result of the direct competition between the perpendicular compression (local concentration) of the ED toward the bond path, as embodied by the two negative curvatures of the ED, $\rho(\mathbf{r})$, at $\mathbf{r}_c$, and the dilatation (local depletion) of the ED in the direction parallel to the path, as embodied by the positive curvature of the ED at $\mathbf{r}_c$. The two negative curvatures of the ED at $\mathbf{r}_c$, $\partial^2\rho(\mathbf{r}_c)/\partial x_1^2$ and $\partial^2\rho(\mathbf{r}_c)/\partial x_2^2$, are denoted λ_1 and λ_2, respectively, and the positive one, $\partial^2\rho(\mathbf{r}_c)/\partial x_3^2$, is denoted λ_3, such that $\lambda_1 + \lambda_2 + \lambda_3$ is equal to the divergence of the gradient of $\rho(\mathbf{r}_c)$, namely the Laplacian $L(\mathbf{r}_c) = \nabla^2\rho(\mathbf{r}_c)$.[3] Bader and Essen[6] have asserted that ED is locally compressed at $\mathbf{r}_c$ perpendicular to the bond path when $L(\mathbf{r}_c) < 0$ and that it is locally distended at $\mathbf{r}_c$ toward the bonded atoms when $L(\mathbf{r}_c) > 0$. In other words, when $L(\mathbf{r}_c) > 0$, the ED is contracted away from $\mathbf{r}_c$ and distended in the direction of the pair, the greater the values of $L(\mathbf{r}_c)$ and $\rho(\mathbf{r}_c)$, the greater shielding of the nuclei of the bonded pair, and the greater the

* Corresponding author. E-mail: gvgibbs@vt.edu.
[†] Department of Geosciences, Virginia Tech.
[‡] University of Arizona.
[§] Department of Chemical Engineering, Virginia Tech.
[||] University of Idaho.
[⊥] Pacific Northwest National Laboratory.

10.1021/jp076396j CCC: $40.75
Published on Web 03/07/2008

local stabilization of the system. On the other hand, on the basis of the local electronic energy density, $H(\mathbf{r}) = G(\mathbf{r}) + V(\mathbf{r})$ [$G(\mathbf{r})$ is the positive definite local kinetic density energy and $V(\mathbf{r})$ is negative definite local potential energy density of a bonded interaction], it is apparent that $H(\mathbf{r})$ is negative when $|V(\mathbf{r})| > G(\mathbf{r})$ and positive when $G(r) > |V(\mathbf{r})|$. As prescribed by Cremer and Kraka,[7] $H(\mathbf{r}_c)$ is negative for a "shared" interaction and positive for a "closed-shell" interaction. Unlike $L(\mathbf{r}_c)$, the sign of which is determined by the local virial expression,[3] the sign and magnitude of $H(\mathbf{r}_c)$ are asserted to be determined by the ED itself, the greater the value of $\rho(\mathbf{r}_c)$, the greater the magnitude of $H(\mathbf{r}_c)$.[8]

With the definition of the bond path and its collateral bond critical point properties,[3] numerous studies of the bonded interactions for a variety of materials[9−11] have not only yielded systematic trends that agree with chemical intuition in cases where bonded interactions are clearly involved, but they have also provided a basis for understanding the connection between the local kinetic and potential energy density properties of the bonded interactions as embodied in the local virial theorem and the local electronic energy density; bond length variations and the stabilization of the bonded interactions; the connection between bond length and Pauling's famous bond strength definition of a bonded interaction; identifying and analyzing weak interactions in nucleic acids[12] and van der Waals molecules;[8] and, among other things, the location of domains ascribed to lone and bond pair electrons, protonization, and the location of H atoms in crystals.[13] In this account, the interactions between the O atoms in silicates will be explored in terms of their O−O bond paths and bond critical point properties and their shared and closed-shell interactions and local energy density properties.

Properties of the Bonded Interactions in Silicates. Well-developed bond paths have been found to exist between each Si atom and its coordinating O atoms in all of the silicate minerals evaluated[13,14] with the software CRYSTAL98[15] and TOPOND.[16] Further, the bond critical point, bcp, properties for the Si−O bonded interactions obtained in the calculations are highly correlated with the experimental bond lengths, R(Si−O). As $\rho(\mathbf{r}_c)$ increases in value, R(Si−O) decreases, $\lambda_{1,2} = 1/2(|\lambda_1 + \lambda_2|)$ (the absolute value of the average of the two negative curvatures of the ED perpendicular to the bond path at $\mathbf{r}_c$), and λ_3 and $L(\mathbf{r}_c)$ each increases in a regular way. Further, properties generated with model experimental ED distributions are comparable with calculated model trends, particularly when the experimental ED was measured with either high-resolution or high-energy synchrotron single-crystal X-ray diffraction methods.[13] The bond paths and the bcp properties for the other first and second row M metal atom M−O bonded interactions in the silicates are comparable with those displayed by the Si−O bonded interactions and show similar trends.[13] As the ED distribution adopts a configuration that yields the lowest energy for a stationary state as a whole, the accumulation of ED density along the bond paths[11] together with the increase in the value of $L(\mathbf{r}_c)$ are asserted to locally stabilize a structure. As the $H(\mathbf{r}_c)$ value for each of the Si−O interactions is negative, collectively they qualify as shared interactions.

The $H(\mathbf{r}_c)$ values for the M−O interactions Be−O, B−O, C−O, Al−O, P−O, and S−O are likewise negative and qualify as shared interactions.[7] Moreover, as $\rho(\mathbf{r}_c)$ increases, $L(\mathbf{r}_c)$ and the ED along the bond path both increase, and the interactions are asserted to become progressively more locally stabilizing as the value of $H(\mathbf{r}_c)$ decreases and becomes progressively more negative.[7] As the $H(\mathbf{r}_c)$ values for the Li−O, Na−O, and Mg−O bonded interactions are each positive, they qualify as closed-shell interactions. But for these interactions, $\rho(\mathbf{r}_c)$ increases rather than decreases in value as the values for $H(\mathbf{r}_c)$ and $L(\mathbf{r}_c)$ both increase. As such, the accumulation of ED along the bond path for a shared or closed-shell interaction is believed to have an impact on the stability;[11] the greater the value of $\rho(\mathbf{r}_c)$ and the accumulation of the ED along the bond path, the larger the value of $L(\mathbf{r}_c)$, the greater the shielding of the nuclei, and the greater the local stabilization the structure. But contrary to the assumption that $\rho(\mathbf{r}_c)$ increases as $H(\mathbf{r}_c)$ decreases, for closed-shell interactions, $H(\mathbf{r}_c)$ actually increases and becomes progressively more positive as $\rho(\mathbf{r}_c)$ increases. Thus, for the closed-shell Li−O, Na−O, and the Mg−O interactions, $\rho(\mathbf{r}_c)$ actually *increases* as $H(\mathbf{r}_c)$ increases, whereas on the contrary, for the shared Be−O, B−O, C−O, Al−O, Si−O, P−O, and S−O interactions, $H(\mathbf{r}_c)$ decreases as $\rho(\mathbf{r}_c)$ and $L(\mathbf{r}_c)$ both increase.

O−O Bond Paths. Bond paths between the O atoms are not rare features in the ED distributions of minerals, as demonstrated by Array and Bader,[17] Gibbs et al.,[18,19] and Luaña et al.,[20] but they are usually not as plentiful nor as robust as those between the metal and oxygen atoms. In this study, the O−O bond paths that span pairs of O atoms in silicates will be examined in terms of their bond critical point properties, their local electronic energies $H(\mathbf{r}_c)$, and the ED distributions associated with the nearby O and M atoms to determine whether they qualify as shared or closed-shell interactions and are locally stabilizing interactions.[7] Trends will be reported in this account between the bcp properties and the separations between the adjacent O atoms, R(O−O), that are comparable with those displayed by the experimental M−O bond lengths, R(M−O), in silicates containing first and second row M-atoms of the periodic table.[14] The evidence will suggest that the bulk of the O−O interactions qualify as closed-shell interactions as observed on the basis of the value and the sign of $L(\mathbf{r}_c)$.[20] In a recent study of the ED distributions for a number of diketone molecules, the bond paths between the O atoms indicate that the O−O interactions for molecules with positive local electronic energy density $H(\mathbf{r}_c)$ values of ∼0.0015 au actually serve to *locally* stabilize the structures by as much as 65 kJ/mol as $L(\mathbf{r}_c)$ and $\rho(\mathbf{r}_c)$ increase, but *globally* the molecules are actually destabilized.[21] These paths occur between the open conformers of the enol isomers with the R(O−O) values close to twice the atomic radius of an O atom. Cioslowski et al.[22−24] argued earlier that this type of bond path, which is associated with a local stabilization in the energy, is indicative of a nonbonded repulsive interaction rather than an attractive one. In contrast, if it were not for their short contacts, the O−O interactions in sterically crowded complexes would probably be described instead as nonbonded rather than locally stabilizing interactions.[23]

Following the criteria set forth by Cremer and Kraka,[7] a shared interaction will be assumed to exist in this account when the value of $H(\mathbf{r}_c)$ is negative for an interaction and a closed-shell one will be assumed when $H(\mathbf{r}_c)$ is positive.[7,8] Upon completing a calculation of the bcp properties for danburite, $CaB_2Si_2O_8$, by means of ab initio perturbed quantum mechanical calculations, Luaña et al.[20] found with their software that 11 O−O bond paths are considered to be secondary (i.e., between second and further nearest neighbor) anion−anion bonds. On the basis of the paths and those found for a relatively large number of other silicates and oxides together with the observation that $L(\mathbf{r}_c) > 0$, they concluded that the O−O bonds in most crystals are clearly secondary closed-shell ionic interactions. An earlier calculation for danburite, using CRYSTAL98[15] and TOPOND[16] software, however, yielded only two O−O paths

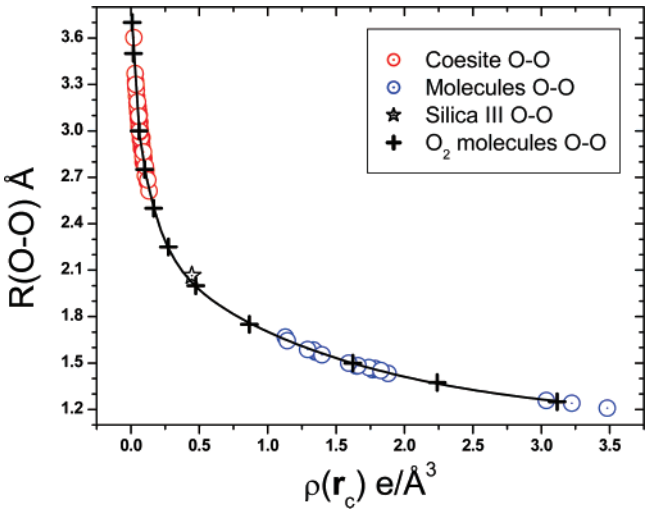

Figure 1. The distances between the O atoms, R(O−O), connected by bond paths for coesite (red circles), calculated at several pressures between 0 and 17.4 GPa, for peroxo and superoxo molecules[18] (blue spheres) and pyrite structure type of silica III (star) determined at 271 GPa and 300 K[32] plotted with respect to the value of the electron density, $\rho(\mathbf{r}_c)$ at the bond critical point. The plus symbols (+) represent the $\rho(\mathbf{r}_c)$ values calculated at the B3LYP/6-311G(2df,p) level for an O_2 molecule as a function of the O−O separation, R(O−O) (Å).

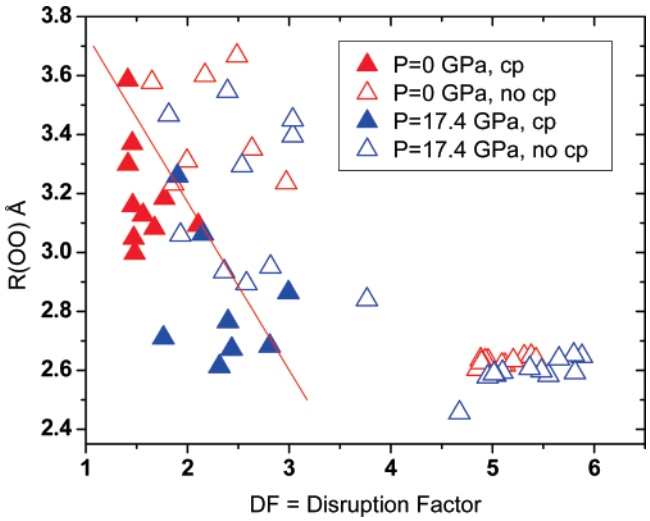

Figure 2. The O−O separations, R(O−O) (Å), calculated for coesite plotted with regard to the disruption factor, DF (adapted from Figure 7, ref 18). The red triangles represent O−O separations calculated for coesite at $P = 0$ GPa and the blue ones represent O−O separations calculated at 17.4 GPa. The solid triangles represent O−O separations connected by bond paths while the open triangles represent O−O separations that lack bond paths. The data include all of the O−O separations in coesite less than or equal to 3.7 Å. The distributions were found to be essentially the same for the O−O separations calculated for coesite at an intermediate pressure. The O−O data that cluster with an R(O−O) value of ∼2.6 Å and DF values ranging between 5 and 6 represent the O atoms that comprise unshared edges of the silicate tetrahedra in coesite.

each with a positive $H(\mathbf{r}_c)$ value, confirming the O−O interactions as closed-shell.[14] In addition, only one path was found for quartz and zero were found for corundum, Al_2O_3, whereas Luaña et al.[20] reported three each for both quartz and corundum.

Disruption Factor and the O−O Bond Paths in Coesite. A geometry optimization of the structure of the high-pressure silica polymorph coesite, undertaken as a function of pressure at absolute zero, using first principles quantum chemical LDA methods, yielded Si−O bond lengths and Si−O−Si angles that agree within a few percent with the experimental values recorded for pressures up to ∼8 GPa.[18] Moreover, the calculated bcp properties for the bonds and angles at $P = 0.0$ GPa are comparable with those determined experimentally.[25] In addition to the bond paths between the Si and O atoms, several paths were also found between the O atoms of the adjacent silicate tetrahedra that persisted to pressures in excess of 10 GPa. The calculated $\rho(\mathbf{r}_c)$ values for the O−O bond paths were found to increase from 0.05 to 0.15 e/Å^3 as values of $L(\mathbf{r}_c)$ increase from 0.60 to 2.05 e/Å^5 and as R(O−O) decreases from 3.15 to 2.60 Å with increasing pressure. For purposes of comparison, the structures of several peroxo- and superoxo-bearing molecules were geometry-optimized at the B3LYP/6-311G(2df,p) level. When the geometry-optimized R(O−O) and $\rho(\mathbf{r}_c)$ values were combined with those calculated for coesite, the values track along the power-law-like R(O−O) vs $\rho(\mathbf{r})$ trend for the O_2 molecule ($^1\Sigma^+$) also calculated at same level (Figure 1). A similar power law trend has also been reported for the O−O interactions for a variety of silicates, oxides, and molecules.[14,20]

As evinced by the figure, the R(O−O)−$\rho(\mathbf{r})$ trend persists for the O_2 molecule for O−O separations in excess of 3.7 Å with the $\rho(\mathbf{r}_c)$ values matching those calculated for coesite at 0.0 and 17.6 GPa and the geometry-optimized peroxo- and superoxo-bearing molecules. The question arises, why are each of the Si atoms in coesite connected to each of its nearest neighbor O atoms by bond paths while there are relatively few O−O bond paths? Perhaps the number of the paths in coesite and other silicates depends at times upon the disruptive impact associated with the superposition of the ED distributions contributed by nearby Si and O atoms. The existence of an O−O path may be expected to depend on both the initial value of $\rho(\mathbf{r})$ at the potential bcp and the extent to which the ED contributed by the nearby metal M atoms like Si in a structure disrupts the ED distribution along the path. That is, the likelihood that a path will possibly survive or will form may depend, at least in part, on the O−O separation, the distance between the potential bcp, and the ED distributions of the nearby M atoms. Taking these factors into account for the potential O−O bond paths in coesite, the following disruption factor model was formulated[18]

$$\mathrm{DF}(p) = \sum q_{\mathrm{Si}}(e^{(2.7-|p-q_{\mathrm{Si}}|-1)}) + \sum q_{\mathrm{O}}(e^{(2.0-|p-q_{\mathrm{O}}|)-1})$$

The value of p denotes the position of the midpoint along the internuclear line for each O−O pair where R(O−O) is less than 3.7 Å. For a particular value of p, the first summation is completed over all of the Si atom positions q_{Si} within a distance of 2.7 Å of p, while the second summation is completed over the O atom positions in the structures q_{O} within a distance of 2.0 Å from the midpoint, excluding the two O atoms involving the pair. The values of the two cutoffs were determined by examining maps of $\rho(\mathbf{r})$ versus the distance between $\mathbf{r}$ and the nucleus of a single Si and a single O atom, respectively. The cutoff values were chosen where the value of $\rho(\mathbf{r})$ adopted a value close to zero.

If the disruption factor, DF, model is befitting and holds, then the data points representing the potential O−O bond paths and bcp points recorded for coesite can be expected to plot in the lower left domain of Figure 2 (adapted from Figure 7, ref 18), the region where the value of DF and the O−O separations, R(O−O), are both relatively small. The red and blue solid triangles represent the midpoints for the O−O separations for which bond paths and bcps were found for coesite, whereas the hollow ones represent the midpoints for the O−O separations

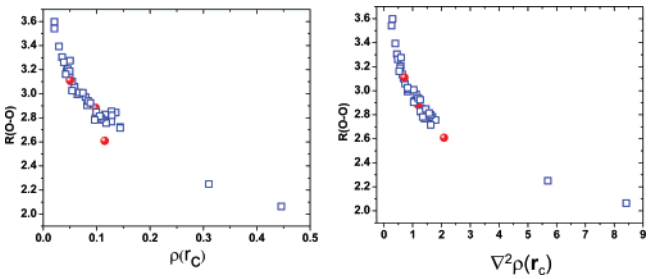

Figure 3. Calculated (blue squares) and observed (red spheres) values of the electron density, $\rho(\mathbf{r}_c)$ (left), and the Laplacian of the electron density, $L(\mathbf{r}_c)$ (right), evaluated at the bond critical points, $\mathbf{r}_c$, for O−O separations in silicates with bond paths plotted with respect to the separation between the O atoms, R(O−O).

that lack bond paths and bcps. The red triangles denote the O−O separations calculated at $P = 0.0$ Gpa, while the blue ones denote the separations calculated at 17.6 GPa. Given that the bulk of the solid red and blue triangles, involving the O−O separations with bond paths and bcps, cluster in the lower left domain of the figure and that the open triangles representing larger O−O separations and DF values plot elsewhere, it is apparent that the clustering of the data in the figure is consistent with the DF model.[26] Indeed, the DF model partitions the O−O separations in coesite into two largely disjoint domains with little overlap, suggesting that the formation or survival of an O−O bond path in coesite is dependent, in part, on the separation between the O atoms and the impact of the ED distribution of the nearby Si atoms on the ED distribution defining the bond path, and of course, on the interaction between the two O atoms. In short, the O−O bond paths that are displayed in coesite are those with relatively small R(O−O) values with bcps that are relatively distant from the Si atoms of the structure. In contrast, the separations between the O atoms comprising the unshared O−O edges of the SiO_4 silicate tetrahedral oxyanions are typically shorter, ∼ 2.6 Å, but as the Si atoms of the two nonequivalent silicate tetrahedra are located ∼0.9 Å from the midpoints of the O−O edges, the DF is large, ranging between 5 and 6 (see Figure 2). As such, despite the short O−O distances, there is an absence of bond paths along the unshared edges of the silicate tetrahedra, a result that is ascribed to the disruptive effect of the Si atoms that center the tetrahedra. Consequently, whether or not a bond path is formed, one might consider the positions of the other atoms in the structure to gauge whether it is likely that the path may also be related to the ED of the nearby bonded atoms or, when bond paths do not emerge, whether an interaction may have been obliterated by the ED distribution of the nearby atoms. On the basis of the local electronic energy density $H(\mathbf{r}_c)$ values (0.0008−0.0011 au) calculated for coesite, the interactions for the O atoms connected by bond paths in coesite qualify as weak closed-shell interactions. In an interesting study of the bonded interactions in DNA, evidence for weak closed-shell O−O interactions was established for representative fragments of the nucleic acid with properties that are comparable with the shorter O−O separations in coesite.[12] Despite the weak nature of the interactions, it was postulated that weak ones like those between the O atoms play an important role in stabilizing the structures of a nucleic acid.

Bond Critical Point Properties for O−O Interactions Displayed by Silicates. When the bcp properties for the M−O interactions for the silicates were originally calculated,[13,14] the bond paths and bcp properties observed for the O−O interactions were ignored, because it was not clear at the time as to their significance, particularly since O−O paths were also displayed by nonstationary state, inert atom procrystal representations of the static ED distributions for the low quartz and coesite structures determined at pressures of ∼6 GPa and higher.[18,19] On the basis of the O−O bond paths with comparable bcp properties for the procrystal representations of the ED for these two silica polymorphs, it was argued that the bond paths and properties, in certain cases, might have little to do with the bonded interactions between the O atoms but more to do with the superposition of the atomic ED distributions of the nearby Si atoms.

The bcp properties for the O−O interactions found for the silicates including quartz and coesite are plotted in Figure 3 with respect to R(O−O). As observed for the M−O bonded interactions, $\rho(\mathbf{r}_c)$ and $L(\mathbf{r}_c)$ each increase with decreasing R(O−O). Also, the trends are comparable with the M−O interactions with similar bond lengths. These results suggest that the bcp properties for the O−O bond paths in the two silica polymorphs behave like M−O interactions. For example, the properties calculated for the K−O bonded interactions of low microcline, $KAlSi_3O_8$, with bond lengths, ranging between 2.76 and 2.98 Å, display properties [$\rho(\mathbf{r}_c) \sim 0.1$ e/Å^3 and $L(\mathbf{r}_c) \sim 1.0$ e/Å^5] that are comparable with those displayed by the O−O interactions. The R(O−O), $\rho(\mathbf{r}_c)$, and $L(\mathbf{r}_c)$ values observed for diopside[27] and $LiGaSi_2O_6$[28] are plotted (red spheres) in Figure 3 for comparison with the calculated trends. The agreement with the calculated bcp properties indicates that the values are considered to be adequate.[10] For the O−O interactions, as observed for the closed-shell M−O interactions, it is notable that, when positive, $H(\mathbf{r}_c)$ increases in value as $\rho(\mathbf{r}_c)$ and $L(\mathbf{r}_c)$ both increase. Not only are the bcp properties for the ubiquitous F−F bond paths in crowded difluorinated aromatic compounds highly correlated with R(F−F), but the F−F interactions also qualify as a closed-shell on the basis of their positive $H(\mathbf{r}_c)$ values. Also, as observed for the closed-shell O−O interactions, $H(\mathbf{r}_c)$ tends to increase in value as both $\rho(\mathbf{r}_c)$ and $L(\mathbf{r}_c)$ increase.[29]

Connection between Bond Paths for Shared O−O Edges and the Disruption Factor. It was suggested in the study of the disruption factor[18] that the formation of an O−O bond path may be related in certain cases to the symmetrical arrangement of a pair of equivalent O−O edge-sharing MO_n coordinated polyhedra (equivalent in the sense of the equivalence relation) with M atoms located on opposite sides of the shared edge. Clearly, the DF model does not take symmetry explicitly into account, but it does suggest that, if M atoms occupy two equivalent or quasiequivalent edge-sharing coordinated polyhedra, the ED associated with the M atoms on opposite sides of the edge may interfere constructively and perhaps result in an enhancement rather than a disruption of the ED along the O−O line. In the case of periclase, several alkali halides, and perovskite, such bond paths and bcps were reported to exist along the shared edges of the equivalent M atom containing coordinated polyhedra.[17,20,30] Bond paths also exist along each of the shared edges of the equivalent and quasiequivalent coordinated polyhedra of both chain silicates diopside [$CaMg(SiO_3)_2$] and tremolite [$Ca_2Mg_5(Si_4O_{11})_2(OH)_2$] (Figure 4, parts a and b, respectively).[14] In the case of diopside, bond paths not only exist along the edges shared by the equivalent MgO_6 octahedra and the equivalent CaO_8 polyhedra but also along the edges shared in common by quasiequivalent MgO_6 and CaO_8 polyhedra. Bond paths also span the edges shared in common by the MgO_6 octahedra in tremolite, including those between the equivalent $M1O_6$ octahedra, but unlike diopside, none spans the edges shared in common with MgO_6 and CaO_8 polyhedra. The calculated $H(\mathbf{r}_c)$ values for tremolite are marginally zero,

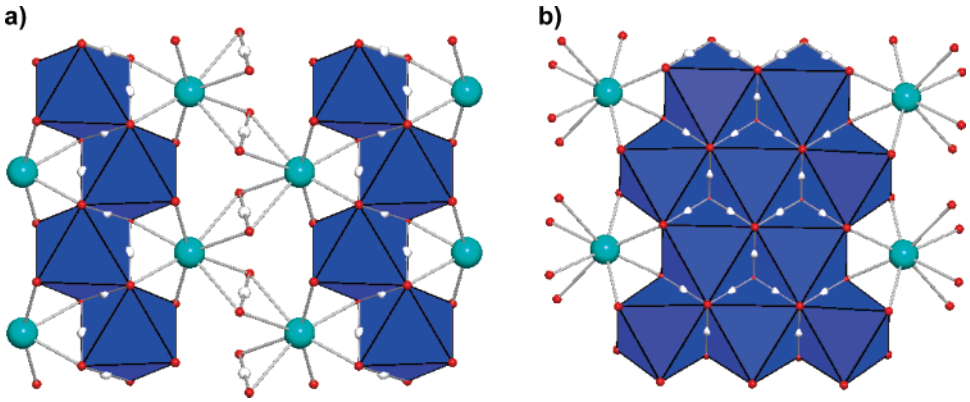

Figure 4. The edge-sharing MgO_6 octahedra and CaO_8 polyhedra in diopside (a) and tremolite viewed down a^* perpendicular to (100). The Mg atoms (not shown) are enclosed in the blue MO_6 octahedra, while the Ca atoms (green spheres) are each bonded to eight O atoms (small red spheres) and comprise the CaO_8 coordinated polyhedra. The bond critical point (bcp) that centers each O−O bond paths is displayed by a small white sphere. Each of the O atoms comprising the edges shared by the equivalent MO_6 octahedra in diopside and tremolite are linked by a bcp centered bond path, and the O atoms comprising the edge-sharing equivalent CaO_8 polyhedra in diopside are likewise connected by bcp centered bond paths. The two edge-sharing $M3O_6$ octahedra in tremolite are equivalent, while the edge-sharing $M1O_6$ and $M2O_6$ octahedra have very similar geometries and are quasiequivalent to the $M3O_6$ octahedra. None of the O atoms comprising the unshared edges of the MO_6 and CaO_8 coordinated polyhedra are connected by bcp centered bond paths.[36]

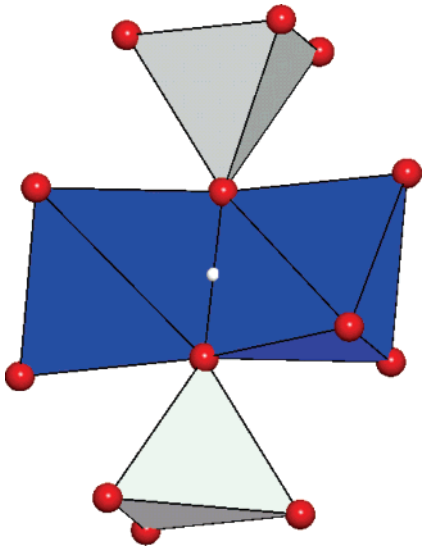

Figure 5. Two equivalent edge-sharing AlO_5 coordinated polyhedra (colored blue) in andalusite where the O3 atoms forming the shared edge are each bonded to a silicate tetrahedral oxyanion (colored gray). The red spheres represent the O3 atoms and the small white one centering the shared edge represents the bcp along the bond path that spans the O atoms that comprise the shared edge. The separation between the O3 atoms in andalusite, 2.250 Å, is the shortest O−O separation reported for a silicate other that reported for silica III, 2.06 Å.[32]

ranging between −0.00006 and 0.00035 au, whereas those calculated for diopside are likewise marginally zero, ranging between −0.00021 and 0.00078 au. Collectively, they indicate that little or no ED is accumulated at the bcps for the shared edge O−O interactions. O−O bond paths also exist in forsterite (Mg_2SiO_4) between equivalent edge-sharing $Mg1O_6$ octahedra and quasiequivalent $Mg1O_6$ and $Mg2O_6$ octahedra. One-quarter of the edges of each FeO_8 coordination polyhedron in almandine garnet ($Fe_3Al_2Si_3O_{12}$) are shared between equivalent FeO_8 polyhedra but with a marginally zero $H(\mathbf{r}_c)$ value of −0.00039 au. The aluminosilicate andalusite (Al_2SiO_5) possesses two equivalent edge-sharing AlO_5 coordination polyhedra (Figure 5) with an O−O separation that is the shortest known shared edge (2.25 Å) in a silicate, which was considered by Burnham and Buerger[31] to be close to the lower limit attainable without the formation of a "homopolar" interaction. Despite the relatively large values of $\rho(\mathbf{r}_c)$ (0.31 e/Å^3) and $L(\mathbf{r}_c)$ (5.7 e/Å^3) calculated for the interaction, the energy density $H(\mathbf{r}_c)$ value is positive (0.0025 au) and substantially larger than that observed for the above silicates, indicating that the interaction is a closed-shell rather than a shared interaction. Like the silica polymorphs, bond paths in the framework silicate beryl [$Al_2(Be_3Si_6O_{18})$] span the bridging O1 and nonbridging O2 atoms of adjacent six-membered rings of silicate tetrahedra. But, unlike the silicates discussed above, the CaO_7 coordinated polyhedra in danburite do not share edges with equivalent CaO_7 polyhedra. In this case, bond paths occur along two of the unshared edges [R(O3−O3) = 2.658 Å, R(O1−O3) = 2.795 Å] of the polyhedra. An examination of the distances of the nearest neighbor Ca, B, and Si atoms from the critical points along the edges shows that these atoms are symmetrically distributed in a triangular array about the critical points each at a distance greater than 2.0 Å. With this exception, none of the O atoms that comprise the unshared edges of MO_n coordinated polyhedra in diopside, tremolite, forsterite, and andalusite are connected by O−O bond paths. Also, no bond paths were found spanning the typically short unshared edges of the BeO_4, BO_4, AlO_4, PO_4, and SO_4 tetrahedral oxyanions for any of the structures for the same reason that none was observed for the SiO_4 tetrahedral oxyanions in coesite and quartz.

To our knowledge, the shortest reported separation between O atoms reported for a silicate exists in the very high-pressure pyrite structure type of silica denoted silica III. In a structural analysis of the silica polymorph, completed at 271 GPa and 300 K, Kuwayama et al.[32] reported an O−O separation of 2.06 Å. But as this separation is substantially longer than that observed for the O_2 molecule (1.21 Å), they concluded that the O atoms are not bonded in the same sense that the S atoms of the S_2 dimer in pyrite (FeS_2) are bonded. A calculation of the ED for silica III, however, displays a well-defined bond path and bcp between the O atoms with $\rho(\mathbf{r}_c) = 0.45$ e/Å^3, $\nabla^2\rho(\mathbf{r}_c) = 8.42$ e/Å^5, and $H(\mathbf{r}_c) = -0.0035$ au. The $\rho(\mathbf{r}_c)$ value plotted with respect to R(O−O) falls close to but slightly displaced from the R(O−O)−$\rho(\mathbf{r}_c)$ curve calculated for the O_2 molecule (Figure 1). On the one hand, the negative $H(\mathbf{r}_c)$ value indicates that the O atom interaction is shared rather than closed-shell. But on the other, Oganov et al.[33] found in a mapping of the $-L(\mathbf{r})$ and the electron localization function (ELF) in a plane containing the O−O path that no maximum in the distribution exists that

could be ascribed to a bonded interaction. Given that the R(O−O) value of the "O_2 dimer" in silica III is substantially longer than that observed for the gas-phase O_2 molecule together with the absence of local ELF and $L(\mathbf{r}_c)$ maxima along the path, they "argued that there are no O−O bonds in the structure". The absence of a maximum along the O−O path cannot, however, be taken as unequivocal evidence for establishing whether a bonded interaction exists between a pair of atoms, because the F_2 molecule, for example, lacks $-L(\mathbf{r}_c)$ and ELF maxima along the F−F bond path.[34] In this case, no one would conclude that the F atoms in the F_2 molecule are not bonded. As the $H(\mathbf{r}_c)$ value for silica III is negative and an order of magnitude larger than that observed above for the closed-shell O−O interactions, the O−O interaction qualifies as a shared interaction. For purposes of comparison, it is noteworthy that the bcp properties and the local electronic energy density for an Al−O bonded interaction in andalusite of the similar length (2.09 Å) are comparable in value with those calculated for the O−O interaction in silica III : $H(\mathbf{r}_c) = -0.0027$ au, $\rho(\mathbf{r}_c) = 0.28$ e/Å^3; $\nabla^2\rho(\mathbf{r}_c) = 4.84$ e/Å^5.

Concluding Remarks

The disruption factor model partitions the O−O separations in coesite into two largely disjoint domains, one with and one without bond paths. As the local electronic energy values are marginally positive, the O−O interactions for the silica polymorph qualify as weak close-shell interactions with the accumulation of the ED along the bond paths serving to locally stabilize the structure marginally relative to one lacking paths. In addition to providing a basis for understanding the presence of bond paths along the unshared edges of the CaO_7 coordinate polyhedra in danburite, the model also provides a basis for understanding why O−O bond paths often occur along the shared edges of MO_n coordinated polyhedra (particularly when $n > 4$) more often than they occur along unshared edges. The ED accumulated along the O−O bond paths of the shared edges of the coordinated polyhedra for forsterite, tremolite, and almandine garnet is also indicated to locally stabilize the structures marginally on the basis of the local electronic energy densities of the weak closed-shell O−O interactions. As the local electronic energy density values for the unusually short O−O shared edge between the AlO_5 coordination polyhedron is positive, the O−O interaction qualifies as a closed-shell interaction. The accumulation of the ED along the shared edges can be considered to stabilize a structure locally by shielding the nuclei of the M atoms comprising the edge-sharing coordinated polyhedra. A fact that contradicts the disruption model is that there are a number of structures with equivalent edge-sharing coordinated polyhedra that lack bond paths. For example, sillimanite (Al_2SiO_5) contains equivalent edge-sharing AlO_6 octahedra and stishovite (SiO_2) contains equivalent edge-sharing SiO_6 octahedra but lacks O−O bond paths.

It is well-known that the shared O−O edges of MO_n coordinated polyhedra are shorter than the unshared ones, a stabilizing feature that Pauling[35] ascribed to cation−cation Coulomb terms. But, if the bond paths between the O atoms represent bonded interactions, then the short nature of the shared edges can arguably be ascribed in part to the bonded interactions between the O atoms. It is notable, however, that the separations between the O atoms comprising shared edges with O−O paths are, on average, virtually the same as those between the shared-edge O atoms that lack paths. As such, it is doubtful whether the interactions between the O atoms have a substantial impact on the length of the O−O interactions, particularly since they qualify as weak closed-shell interactions. In contrast, the O atoms comprising the O_2 dimer in silica III qualifies as a shared interaction.

Acknowledgment. The National Science Foundation and the U.S. Department of Energy are thanked for supporting this study with grants EAR-0609885 (N.L.R. and G.V.G.), EAR-0609906 (R.T.D.), and DE-FG02-97ER14751 (D.F.C.). K.M.R. acknowledges a grant from the U.S. Department of Energy (DOE), Office of Basic Energy Sciences, Geosciences Division and computational facilities and support from the Environmental Molecular Sciences Laboratory (EMSL) at the Pacific Northwest National Laboratory (PNNL). The computations were performed in part at the EMSL at PNNL. The EMSL is a national scientific user facility sponsored by the U.S. DOE Office of Biological and Environmental Research. PNNL is operated by Battelle for the DOE under Contract DE-AC06-76RLO 1830. G.V.G. takes pleasure in thanking Bob Downs for providing support for his visit to the University of Arizona during the winter of 2007, where a portion of the manuscript was written. He also takes great pleasure in thanking an unknown reviewer for an excellent review of an earlier version of the manuscript, bringing to his attention the absence of $-L(\mathbf{r}_c)$ maxima connecting the clearly bonded F atoms of the F_2 dimer, among other things, that led to substantial improvements. My good friend and colleague Richard Bader is also thanked for reviewing the manuscript and making a number of valuable suggestions in an early version of the manuscript.

References and Notes

(1) Cioslowski, J.; Mixon, S. T.; Edwards, W. D. *J. Am. Chem. Soc.* **1991**, *113*, 1083.
(2) Runtz, G. R.; Bader, R. F. W.; Messer, R. R. *Can. J. Chem.-Rev. Can. Chim.* **1977**, *55*, 3040.
(3) Bader, R. F. W. *Atoms in Molecules*; Oxford Science Publications: Oxford, UK, 1990.
(4) Bader, R. F. W. *Acc. Chem. Res.* **1985**, *18*, 9.
(5) Bader, R. F. W. *J. Phys. Chem. A* **1998**, *102*, 7314.
(6) Bader, R. F. W.; Essen, H. *J. Chem. Phys.* **1984**, *80*, 1943.
(7) Cremer, D.; Kraka, E. *Croat. Chem. Acta* **1984**, *57*, 1259.
(8) Bone, R. G. A.; Bader, R. F. W. *J. Phys. Chem.* **1996**, *100*, 10892.
(9) Bader, R. F. W. *Chem. Rev.* **1991**, *91*, 893.
(10) Koritsanszky, T. S.; Coppens, P. *Chem. Rev.* **2001**, *101*, 1583.
(11) Gatti, C. *Z. Kristallogr.* **2005**, *220*, 399.
(12) Matta, C. F.; Castillo, N.; Boyd, R. J. *J. Phys. Chem. B* **2006**, *110*, 563.
(13) Gibbs, G. V.; Downs, R. T.; Cox, D. F.; Ross, N. L.; Prewitt, C. T.; Rosso, K. M.; Lippmann, T.; Kirfel, A. *Z. Kristallogr.* **2008**, In Press.
(14) Gibbs, G. V.; Boisen, M. B.; Beverly, L. L.; Rosso, K. M. A computational quantum chemical study of the bonded interactions in earth materials and structurally and chemically related molecules. In *Molecular Modeling Theory: Applications in the Geosciences*; Cygan, R. T., Kubicki, J. D., Eds.; Mineralogical Society of America: Washington, DC, 2001; Vol. 42; pp 345.
(15) Saunders, V. R.; Dovesi, R.; Roetti, C.; Causa, M.; Harrison, N. M.; Orlando, R.; Apra, E. CRYSTAL98 User's Manual; University of Torino: Torino, Italy, 1998.
(16) Gatti, C. TOPOND96 User's Manual; CNR-CSRSRC: Milano, Italy, 1997.
(17) Aray, Y.; Bader, R. F. W. *Surf. Sci.* **1996**, *351*, 233.
(18) Gibbs, G. V.; Boisen, M. B.; Rosso, K. M.; Teter, D. M.; Bukowinski, M. S. T. *J. Phys. Chem. B* **2000**, *104*, 10534.
(19) Gibbs, G. V.; Rosso, K. M.; Teter, D. M.; Boisen Jr, M. B.; Bukowinski, M. S. T. *J. Mol. Struct.* **1999**, *485−486*, 13.
(20) Luana, V.; Costales, A.; Mori-Sanchez, P.; Pendas, A. M. *J. Phys. Chem. B* **2003**, *107*, 4912.
(21) Pakiari, A. H.; Eskandari, K. *J. Mol. Struct.−THEOCHEM* **2007**, *806*, 1.
(22) Cioslowski, J. *J. Am. Chem. Soc.* **1990**, *112*, 6536.
(23) Cioslowski, J.; Mixon, S. T. *J. Am. Chem. Soc.* **1992**, *114*, 4382.
(24) Cioslowski, J.; Mixon, S. T.; Fleischmann, E. D. *J. Am. Chem. Soc.* **1991**, *113*, 4751.
(25) Gibbs, G. V.; Whitten, A. E.; Spackman, M. A.; Stimpfl, M.; Downs, R. T.; Carducci, M. D. *J. Phys. Chem. B* **2003**, *107*, 12996.

(26) Kirfel, A.; Gibbs, G. V. *Phys. Chem. Miner.* **2000**, *27*, 270.
(27) Bianchi, R.; Forni, A.; Oberti, R. *Phys. Chem. Miner.* **2005**, *32*, 638.
(28) Bianchi, R.; Forni, A.; Cámara, F.; Oberti, R.; Ohashi, H. *Phys. Chem. Miner*.
(29) Matta, C. F.; Castillo, N.; Boyd, R. J. *J. Phys. Chem. A* **2005**, *109*, 3669.
(30) Abramov, Y. A. *Acta Crystallogr.* **1997**, *A53*, 264.
(31) Burnham, C. W.; Buerger, M. J. *Z. Kristallogr.* **1961**, *115*, 269.
(32) Kuwayama, Y.; Hirose, K.; Sata, N.; Ohishi, Y. *Science* **2005**, *309*, 923.
(33) Oganov, A. R.; Gillan, M. J.; Price, G. D. *Phys. Rev. B* **2005**, *71*, 064104.
(34) Cremer, D.; Kraka, E. *Angew. Chem.-Int. Ed. Engl.* **1984**, *23*, 627.
(35) Pauling, L. *J. Am. Chem. Soc.* **1929**, *51*, 1010.
(36) Gibbs, G. V.; Cox, D. F.; Ross, N. L.; Crawford, T. D.; Burt, J. B.; Rosso, K. M. *Phys. Chem. Miner.* **2005**, *32*, 208.